

## Preparation and mechanical properties of Fe<sub>3</sub>Al/ Al<sub>2</sub>O<sub>3</sub> nano- / micro-composite<sup>①</sup>

YIN Yan-sheng(尹衍升), GONG Hong-yu(龚红宇), FAN Run-hua(范润华),  
WANG Xin(王昕), TAN Xun-yan(谭训彦)

(Key Laboratory for Material Liquid Structure and Heredity of Education Ministry,  
Key Laboratory for Engineering Ceramics of Shandong Province, Shandong University, Ji nan 250061, China)

**Abstract:** Al<sub>2</sub>O<sub>3</sub> matrix composites reinforced with Fe<sub>3</sub>Al nano-particles were fabricated by hot processing at 1 450 - 1 600 °C. The effect of Fe<sub>3</sub>Al content on the densification, mechanical properties and microstructure of the composites was investigated. The results show that some elongated Al<sub>2</sub>O<sub>3</sub> grains are observed. Fe<sub>3</sub>Al particles are mainly situated at grain boundaries of the matrix while smaller particles are trapped within the alumina grains. The addition of Fe<sub>3</sub>Al nanoparticles improves the mechanical properties of alumina. The maximum strength and toughness of the Fe<sub>3</sub>Al/ Al<sub>2</sub>O<sub>3</sub> nanocomposites are 832 MPa and 7.96 MPa·m<sup>1/2</sup>, respectively.

**Key words:** alumina; iron aluminide(Fe<sub>3</sub>Al); composite

**CLC number:** TB 33

**Document code:** A

### 1 INTRODUCTION

Alumina(Al<sub>2</sub>O<sub>3</sub>) ceramics are often considered for structural applications, due to their properties of high hardness, chemical and wear resistance and good mechanical properties at room and high temperature. The well known limitation for these ceramics, however, is the very low toughness. Recent studies have shown significant improvements in mechanical properties, including toughness, by adding ductile second phase particles, such as Ni, Al, Mo and Cu<sup>[1-4]</sup>. An increase of 80% - 333% in the fracture toughness has been reported for Al<sub>2</sub>O<sub>3</sub> with 20% Ni(volume fraction). The toughening mechanisms are crack bridging, crack deflection and network microstructure of Ni existed on Al<sub>2</sub>O<sub>3</sub> grain boundary<sup>[1]</sup>. However, the presence of metallic particles degrades high temperature strength and oxidation resistance because of low melting point of metallic phases and poor wettability between metals and ceramics. Intermetallics have high melting point<sup>[5, 6]</sup>. They are also potential reinforcing phase of Al<sub>2</sub>O<sub>3</sub>, and have better chemical inertance and oxidation resistance than most metals have. Tuan et al<sup>[7, 8]</sup> researched the NiAl/Al<sub>2</sub>O<sub>3</sub> composites containing 0 - 100% NiAl. In their work, the strength increased by 60% and the fracture toughness increased by 160% for the Al<sub>2</sub>O<sub>3</sub> with 50% NiAl(volume fraction). ZHANG et al<sup>[9]</sup> observed an increase in strength and toughness by 39% and 42%, respectively, for Al<sub>2</sub>O<sub>3</sub> with 40% Fe<sub>3</sub>Al which has

been used as cutting tool.

The mechanical properties of composites are known to be improved significantly when the size of dispersing particles is reduced from micrometer to nanometer. The most significant achievements with this approach have been reported by Niihara who firstly revealed that a dispersion of 5% SiC(volume fraction) nanoparticles into Al<sub>2</sub>O<sub>3</sub> increased the room-temperature strength from 350 MPa to 1.0 GPa, accompanied with the fracture toughness increasing from 3.25 MPa·m<sup>1/2</sup> to 4.7 MPa·m<sup>1/2</sup>. Proposed toughening mechanisms included crack deflection and microcracking induced by thermal expansion mismatch between the particles and the matrix grains<sup>[10]</sup>.

The purpose of the present study is to fabricate Fe<sub>3</sub>Al/Al<sub>2</sub>O<sub>3</sub> nanocomposites. The mechanical properties and microstructure are also investigated.

### 2 EXPERIMENTAL

Commercial  $\alpha$ -Al<sub>2</sub>O<sub>3</sub> powder(Zhangjiakou East Special Ceramic Material Co, LTD, China) with an average grain size of 3  $\mu$ m was used as matrix. Fe<sub>3</sub>Al nano-powder was prepared by H<sub>2</sub>-arc plasma technique, and mean particle diameter was 50 nm<sup>[11]</sup>. 5% - 30% (mass fraction) of Fe<sub>3</sub>Al nanoparticles were added to the starting Al<sub>2</sub>O<sub>3</sub> powder. The mixture was ultrasonically dispersed and then ball-milled in ethanol for 1h. The slurry was dried in vacuum and then

① **Foundation item:** Project(50242008) supported by the National Natural Science Foundation of China and project(Y2001F01) supported by the Natural Science Foundation of Shandong Province, China

**Received date:** 2002 - 12 - 24; **Accepted date:** 2003 - 05 - 06

**Correspondence:** YIN Yan-sheng, Professor; E-mail: yys3001@sina.com

passed through sieves to get powders  $\leq 75 \mu\text{m}$ . The mixed powders were placed into a graphite die and hot pressed under 30 MPa in a flowing nitrogen atmosphere at 1 450 °C–1 600 °C for 30 min. For the sake of comparison, a monolithic alumina specimen was hot pressed at 1 530 °C for 30 min. The dimension of the hot pressed specimen was  $d 42 \text{ mm} \times 5 \text{ mm}$ .

Density measure of the as-sintered samples was using the Archimedes' method. Phase identification was performed by X-ray diffraction analysis (XRD, D/max-rA, Japan) with CuK $\alpha$  radiation. Rockwell hardness (HRA) was tested. Microstructure of the composites and crack propagation behavior were observed by scanning electron microscopy (SEM, Hitachi S-2500, Japan). Microstructural characteristics were further examined by transmission electron microscopy (TEM, Hitachi S-800, Japan). Grain size was estimated by line intercept method. The sintered specimens were cut with a diamond saw and ground into 2 mm  $\times$  4 mm  $\times$  36 mm and 3 mm  $\times$  4 mm  $\times$  36 mm for determination of fracture toughness and bending strength, respectively. The fracture toughness,  $K_{IC}$  was measured by single-edge notch beam (SENB, the notch width of 0.25 mm and the depth of 2 mm) method. Bending strength was measured by three point bend method. The cross head speed was 0.5 mm/min with a span of 20 mm. The bending strength and toughness reported for each sample were the average values of 6–8 specimens.

### 3 RESULTS AND DISCUSSION

The XRD pattern for an Fe<sub>3</sub>Al/Al<sub>2</sub>O<sub>3</sub> composite after hot pressing is shown in Fig. 1. The XRD analysis indicates that no phase other than Fe<sub>3</sub>Al and  $\alpha$ -Al<sub>2</sub>O<sub>3</sub> is produced after the hot pressing.

Fig. 2 and Fig. 3 show the SEM photograph of polished surface and the TEM micrograph of 5% Fe<sub>3</sub>Al/Al<sub>2</sub>O<sub>3</sub> composite hot pressed at 1 530 °C, re-

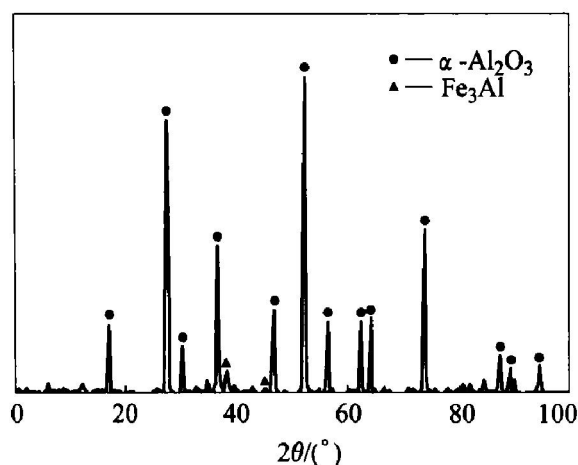


**Fig. 1** XRD pattern for 5% Fe<sub>3</sub>Al/Al<sub>2</sub>O<sub>3</sub> composite after hot pressing at 1 530 °C

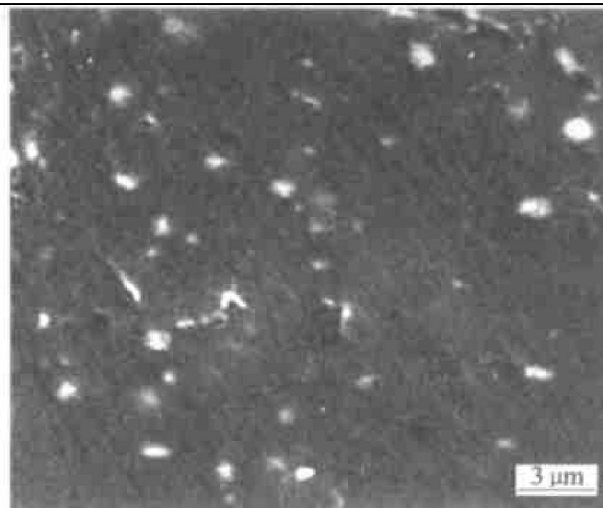


**Fig. 2** SEM morphology of polished surface of 5% Fe<sub>3</sub>Al/Al<sub>2</sub>O<sub>3</sub> composite sintered at 1 530 °C

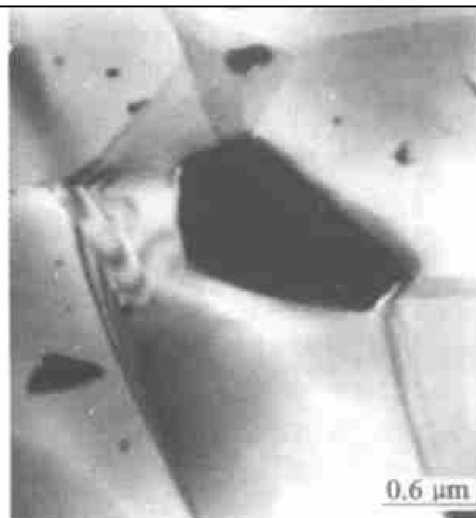


**Fig. 3** TEM micrograph of 5% Fe<sub>3</sub>Al/Al<sub>2</sub>O<sub>3</sub> composite sintered at 1 530 °C

spectively.

Fe<sub>3</sub>Al particles appear a white contrast in SEM micrograph, but dark contrast in TEM micrograph. In the composite, the Fe<sub>3</sub>Al particles were uniformly dispersed in Al<sub>2</sub>O<sub>3</sub> matrix. Many large ones of 600 nm in average size were observed at grain boundaries, and some nano-Fe<sub>3</sub>Al particles were found to be embedded in the matrix grains. Grain size of the intra-granular particles varied from several to several hundred nanometers.

The relative density of monolithic Al<sub>2</sub>O<sub>3</sub> sintered at 1 530 °C is 98.3%, which notes that the ceramic has compacted. Fig. 4 shows the relative density of the composites containing 5%, 10%, 20% and 30% nano-Fe<sub>3</sub>Al particles (noted as FA5, FA10, FA20, FA30) changed with the sintering temperature. The relative density increased with the increase of sintering temperature, but decreased with the increase of Fe<sub>3</sub>Al contents. At 1 560 °C the densities of FA5, FA10 and FA30 were 99.4%, 98.3% and 88%, respectively. At

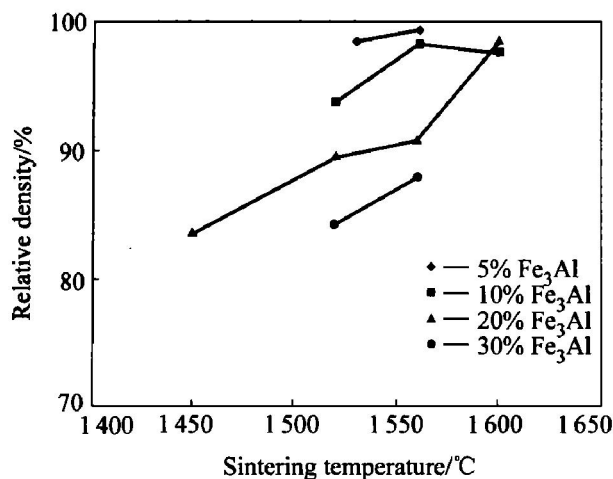


**Fig. 4** Relative densities of  $\text{Fe}_3\text{Al}/\text{Al}_2\text{O}_3$  composites with different  $\text{Fe}_3\text{Al}$  contents at different sintering temperatures

1 530 °C, the density of FA5 was 98.6%. To get the same density, FA10 and FA20 needed to be sintered at 1 560 °C and 1 600 °C. The second phase of nano- $\text{Fe}_3\text{Al}$  inhibits the densification of  $\text{Al}_2\text{O}_3$  matrix.

As shown in Fig. 5, the Rockwell hardness (HRA) of the composite is the function of  $\text{Fe}_3\text{Al}$  contents and sintering temperature. Compared with Fig. 4, the variation of the hardness with

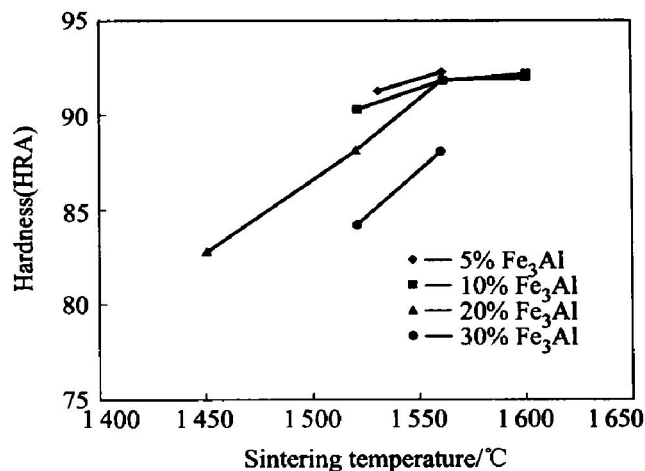


**Fig. 5** Variation of hardness of  $\text{Fe}_3\text{Al}/\text{Al}_2\text{O}_3$  nanocomposites with variable  $\text{Fe}_3\text{Al}$  contents at different sintering temperatures

$\text{Fe}_3\text{Al}$  content and sintering temperature is similar to that of the relative density of the composite, implying the dependence of hardness on the densification of  $\text{Al}_2\text{O}_3$  matrix. The highest hardness value of the composites is HRA 92.

Fig. 6 shows SEM fractographs of the  $\text{Al}_2\text{O}_3$  and the  $\text{Fe}_3\text{Al}/\text{Al}_2\text{O}_3$  nanocomposites. The microstructure of monolithic  $\text{Al}_2\text{O}_3$  sintered at 1 530 °C is characterized by platelet-shaped grains with an

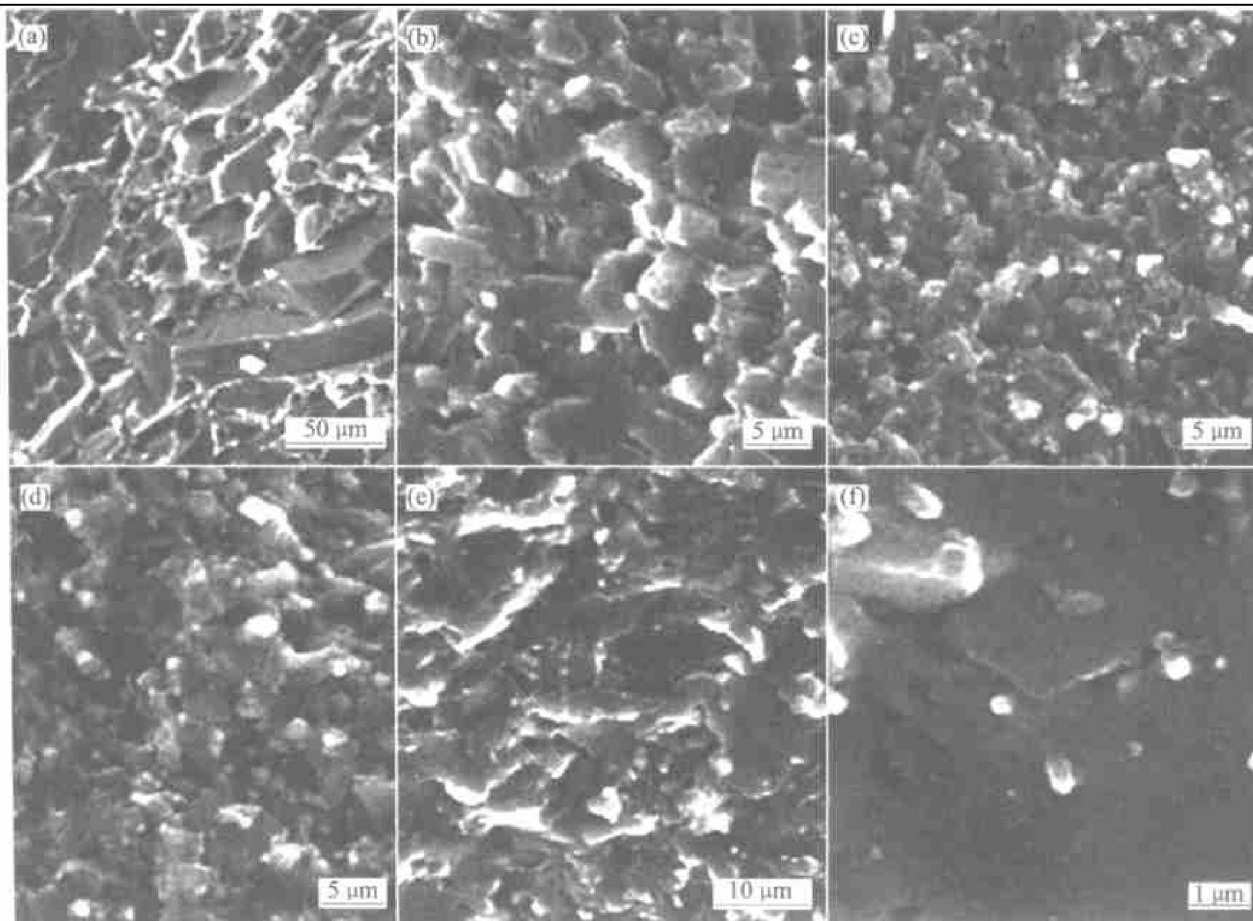


**Fig. 6** SEM fractographs of monolithic  $\text{Al}_2\text{O}_3$  and  $\text{Fe}_3\text{Al}/\text{Al}_2\text{O}_3$  composites sintered at different temperatures  
 (a) —Monolithic  $\text{Al}_2\text{O}_3$ , 1 530 °C; (b) —5%  $\text{Fe}_3\text{Al}/\text{Al}_2\text{O}_3$ , 1 530 °C; (c) —10%  $\text{Fe}_3\text{Al}/\text{Al}_2\text{O}_3$ , 1 520 °C;  
 (d) —20%  $\text{Fe}_3\text{Al}/\text{Al}_2\text{O}_3$ , 1 520 °C; (e) and (f) —10%  $\text{Fe}_3\text{Al}/\text{Al}_2\text{O}_3$ , 1 600 °C

aspect ratio of 4.2 and with average size of 91  $\mu\text{m}$ . The grains of the nanocomposites are smaller and less anisotropic, with an average size of about 8  $\mu\text{m}$ . The phenomenon of the preferential growth of Al<sub>2</sub>O<sub>3</sub> grains has been well investigated<sup>[11]</sup>. The nonuniformly distributed aluminosilicate glassy phase in Al<sub>2</sub>O<sub>3</sub> grain boundaries, caused by small amounts of impurities of the original material, attributed to the anisotropic morphology<sup>[11]</sup>.

In the composite containing 5% Fe<sub>3</sub>Al sintered at 1530 °C, the elongated Al<sub>2</sub>O<sub>3</sub> grains with an average size of 12  $\mu\text{m}$  and approximated aspect ratio of 3.2 (Fig. 6(b)) are smaller than those of monolithic Al<sub>2</sub>O<sub>3</sub>. The fracture mode includes intergranular and transgranular. With the increase of Fe<sub>3</sub>Al nano-particles, the grain size and aspect ratio of the matrix decreased. In 20% Fe<sub>3</sub>Al/Al<sub>2</sub>O<sub>3</sub> composite sintered at 1520 °C, the elongated grains were hardly to be found (Fig. 6(d)). The composite had high porosity, showing intergranular fracture. This indicated that the addition of Fe<sub>3</sub>Al nano-particles result in grain-growth inhibition of the Al<sub>2</sub>O<sub>3</sub> matrix. At higher Fe<sub>3</sub>Al contents and sintering temperatures, slight grain growth of Al<sub>2</sub>O<sub>3</sub> and the coalescence of Fe<sub>3</sub>Al particles at the Al<sub>2</sub>O<sub>3</sub> grain boundaries were observed.

The bending strength and fracture toughness of the monolithic Al<sub>2</sub>O<sub>3</sub> sintered at 1530 °C are 359 MPa and 4.6 MPa·m<sup>1/2</sup>, respectively. Fig. 7 illustrates  $K_{IC}$  and bending strength of the Fe<sub>3</sub>Al/Al<sub>2</sub>O<sub>3</sub> nanocomposite versus the Fe<sub>3</sub>Al content and hot pressing temperature. On the whole, these mechanical properties were increased by addition of Fe<sub>3</sub>Al particles. Bending strength of the 5% Fe<sub>3</sub>Al/Al<sub>2</sub>O<sub>3</sub> composite sintered at 1530 °C was 666 MPa, which was 1.8 times higher than that of the monolithic Al<sub>2</sub>O<sub>3</sub> prepared under the same conditions. When the hot pressing temperature was increased to 1560 °C, the bending strength of FA5 increased to a maximum value of 832 MPa, whereas the strengths of FA10 and FA20 were 722 MPa and 701 MPa, respectively. Consequently, strengthening of the composite was assumed to be attributed to the fine microstructure and the densification of the composite. At 1560 °C, the fracture toughness of the composite with 5% Fe<sub>3</sub>Al was 7.34 MPa·m<sup>1/2</sup>, and those of FA10 and FA20 were slightly higher. When hot pressing temperature was elevated to 1600 °C, the fracture toughness of FA10 increased to 7.96 MPa·m<sup>1/2</sup>, but the value of FA20 decreased to 5.87 MPa·m<sup>1/2</sup>.

The crack propagation behavior around the Vickers indentation for the 5% Fe<sub>3</sub>Al/Al<sub>2</sub>O<sub>3</sub> composite sintered at 1560 °C is shown in Fig. 8. The cracks propagated with large deflection around the Fe<sub>3</sub>Al particles and the in-situ formed platelet Al<sub>2</sub>O<sub>3</sub> grains. The pull-out of the elongated grains

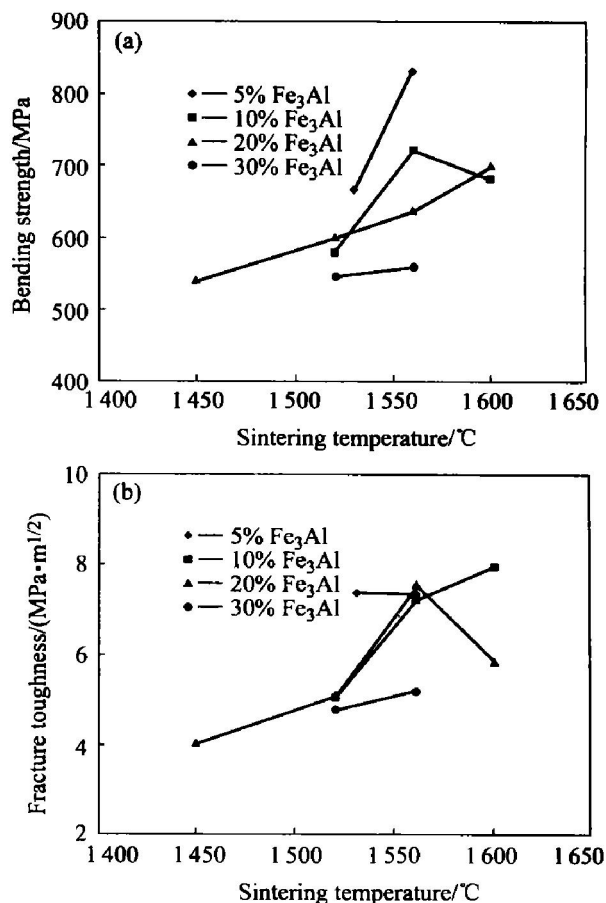


**Fig. 7** Variation of bending strength(a) and fracture toughness( $K_{IC}$ , b) of Fe<sub>3</sub>Al/Al<sub>2</sub>O<sub>3</sub> nanocomposite with sintering temperature and Fe<sub>3</sub>Al content

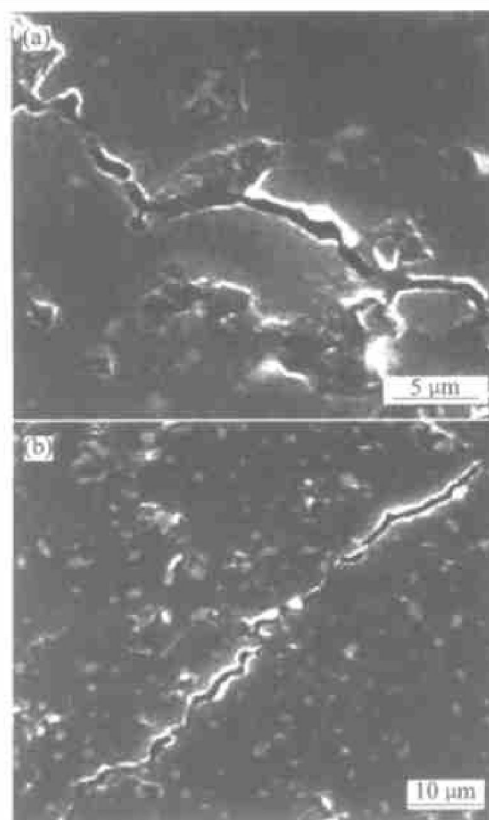


**Fig. 8** SEM photographs of indentation crack propagation of nanocomposites  
(a) —5% Fe<sub>3</sub>Al/Al<sub>2</sub>O<sub>3</sub>, 1530 °C;  
(b) —10% Fe<sub>3</sub>Al/Al<sub>2</sub>O<sub>3</sub>, 1600 °C

was found. In addition, crack penetration through the coalesced  $\text{Fe}_3\text{Al}$  particles and crack-bridging by the elongated  $\text{Al}_2\text{O}_3$  grains were observed. The crack path is thus erratic, and the toughness of the composites is therefore enhanced. The crack path was almost straight in FA10 sintered at  $1600^\circ\text{C}$ , even though the crack deflection and bridging of the  $\text{Fe}_3\text{Al}$  intermetallic particles were found. From the SEM fractograph of the composite, no elongated grains was found (Fig. 6(e)). The high fracture toughness likely results from fine grain. At a higher magnification the fracture surface of FA10 shows many  $\text{Fe}_3\text{Al}$  nanoparticles trapped in the grains of the matrix (Fig. 6(f)). This microstructure was believed to be helpful to strengthening grain boundaries<sup>[11]</sup>. Thus, the cracks are forced to deflect into  $\text{Al}_2\text{O}_3$  grains. Transgranular fracture is the main reason for its high toughness.

#### 4 CONCLUSIONS

1) 5%–30% (mass fraction)  $\text{Fe}_3\text{Al}/\text{Al}_2\text{O}_3$  nanocomposites are successfully fabricated by hot pressing under  $\text{N}_2$  atmosphere. In these composites, nanometer  $\text{Fe}_3\text{Al}$  particles are dispersed within the  $\text{Al}_2\text{O}_3$  grains, and relatively large  $\text{Fe}_3\text{Al}$  particles with about 600nm, are found at the grain boundary.

2) The addition of  $\text{Fe}_3\text{Al}$  particles result in the grain growth inhibition of the  $\text{Al}_2\text{O}_3$  matrix and make the densification of the composite be difficult. The platelet  $\text{Al}_2\text{O}_3$  grains are found in the composites. With the increase of  $\text{Fe}_3\text{Al}$  content, the aspect ratio and grain size of the elongated grains decrease.

3) The highest value of bending strength and fracture toughness of  $\text{Fe}_3\text{Al}/\text{Al}_2\text{O}_3$  nanocomposites are 832 MPa and  $7.96 \text{ MPa} \cdot \text{m}^{1/2}$ , respectively. The strengthening mechanism is attributed to the fine microstructure and densification of the composites. The enhancement of toughness of the composite containing 5%  $\text{Fe}_3\text{Al}$  is due to the crack deflection and bridging effect of  $\text{Fe}_3\text{Al}$  as well as the pull-out effect of the e-

longated  $\text{Al}_2\text{O}_3$  grains. In addition, the transgranular fracture caused by fine grain microstructure is the main reason for the high toughness of 10%  $\text{Fe}_3\text{Al}/\text{Al}_2\text{O}_3$  nanocomposite.

#### REFERENCES

- [1] XU Dong-sun, Yeomans J A. Microstructure and fracture toughness of nickel particle toughened alumina matrix composites[J]. J Mater Sci, 1996, 31: 875–880.
- [2] Loehman R E, Ewsuk K, Tomsia A P. Synthesis of  $\text{Al}_2\text{O}_3$ -Al composites by reactive melt penetration[J]. J Am Ceram Soc, 1996, 79: 27–32.
- [3] Aldrich D E, Edirisinghe M T. Addition of copper particles to alumina matrix[J]. Journal of Materials Science Letters, 1998, 17(12): 965–967.
- [4] Guichard J L, Tillement O, Mocellin A. Alumina-chromium cermets by hot pressing of nanocomposites[J]. J Eur Ceram Soc, 1998, 18: 1743–1752.
- [5] CHEN Yirong, KONG Far-tao, TIAN Jing, et al. Recent developments in engineering  $\gamma$ -TiAl intermetallic [J]. Trans Nonferrous Met Soc China, 2002, 12(4): 610–614.
- [6] ZHENG Wei-wei, YANG Wang-yue, SUN Zu-qing. Anisotropic plastic deformation behavior of B2-ordered  $\text{Fe}_3\text{Al}$  single crystals at room temperature [J]. Trans Nonferrous Met Soc China, 2002, 12(4): 669–675.
- [7] Tuan W H. Toughening alumina with nickel aluminide inclusions[J]. J Eur Ceram Soc, 2000, 20: 895–899.
- [8] Chou W B, Tuan W H, Chang S T. Preparation of NiAl toughened  $\text{Al}_2\text{O}_3$  by vacuum hot pressing[J]. British Ceramic Transactions, 1996, 95(2): 71–74.
- [9] ZHANG Y J, YIN Y S, ZHOU Y. Microstructure and mechanical properties of Fe-Al intermetallic compounds/ $\text{Al}_2\text{O}_3$  composites manufactured by hot pressing[J]. Inter-ceram, 2000, 49(1): 36–39.
- [10] Niihara K. New design concept of structural ceramics: nanocomposites[J]. J Ceram Soc Jpn, 1991, 99(10): 974–982.
- [11] Kebbede A, Paria J, Carim A H. Anisotropic grain growth in  $\alpha$ - $\text{Al}_2\text{O}_3$  with  $\text{SiO}_2$  and  $\text{TiO}_2$  addition[J]. J Am Ceram Soc, 2000, 83(11): 2845–51.

(Edited by YANG Bing)